Nuclear Materials and Energy 2 (2015) 12–19

Contents lists available at ScienceDirect

Nuclear Materials and Energy

journal homepage: www.elsevier.com/locate/nme

Conceptual study of ferromagnetic pebbles for heat exhaust in fusion reactors with short power decay length

N. Gierse [a], J.W. Coenen [a], C. Thomser [b,*], A. Panin [a], Ch. Linsmeier [a], B. Unterberg [a], V. Philipps [a]

[a] Forschungszentrum Jülich GmbH, Institut für Energie- und Klimaforschung - Plasmaphysik, 52425 Jülich, Germany
[b] Forschungszentrum Jülich GmbH, Institut für Energie- und Klimaforschung - Werkstoffstruktur und -eigenschaften, 52425 Jülich, Germany

ARTICLE INFO

Article history:
Received 13 October 2014
Received in revisd form 12 January 2015
Accepted 21 January 2015
Available online 13 April 2015

ABSTRACT

Ferromagnetic pebbles are investigated as high heat flux ($q_{\parallel}$) plasma facing components in fusion devices with short power decay length (λ_q) on a conceptual level. The ability of a pebble concept to cope with high heat fluxes is retained and extended by the acceleration of ferromagnetic pebbles in magnetic fields. An alloying concept suited for fusion application is outlined and the compatibility of ferromagnetic pebbles with plasma operation is discussed.

Steel grade 1.4510 is chosen as a well characterized candidate material to perform an analysis of the heating process. Scaling relationships as a function of $q_{\parallel}$ for maximum and optimal pebble diameter, allowed exposure time, and removal time safety margin are obtained numerically for spherical pebble geometry. The acceleration of ferromagnetic pebbles in a tokamak resulting from magnetic gradients is studied and operation parameters for an ITER-based reactor are outlined. Counter-intuitively, it is found that ferromagnetic pebbles perform better for narrow λ_q profiles, making them an attractive heat exhaust concept for next step devices and thus an option to be investigated in detail.

The key results of this study are that very high heat fluxes are accessible in the operation space of ferromagnetic pebbles, that ferromagnetic pebbles are compatible with tokamak operation and current divertor designs, that the heat removal capability of ferromagnetic pebbles increases as λ_q decreases and, finally, that for fusion relevant values of $q_{\parallel}$ pebble diameters below 100 μm are required.

1. Introduction

Power and particle exhaust are crucial for the viability of any future fusion power plant concept. Heat in fusion reactors must be extracted through a wall and cannot be exhausted volumetrically, which limits the allowed power density in fusion reactors [1] and is a severe technical challenge in itself [2]. In addition, structural material changes resulting from neutron irradiation cause degradation in the heat exhaust capabilities of existing designs [3] and static surfaces can suffer severely from erosion due to impinging plasma particles [4,5]. It is concluded that conventional concepts and materials for plasma facing components (PFCs) reach their limits in terms of material lifetime and power exhaust at approximately 20 MW/m^2, which is presumably dramatically reduced to <10 MW/m^2 due to neutron damage in a D-T reactor [6] or even only half that value [7].

Power exhaust and material lifetime have been identified as a key challenge for next step devices [8]. Recent multi-machine studies show that the power decay length λ_q for attached type-I ELMy H-modes does not scale with the major radius in tokamaks [9]. This can severely strain existing concepts. For ITER, where $\lambda_q \approx 1$ mm is predicted from multi-machine scaling, heat fluxes $q_{\parallel} \sim 200$ MW/m^2 for attached plasma operation must be considered. So far, the impinging heat flux onto the PFCs is reduced by magnetic flux expansion, partial conversion of parallel heat flux to isotropic radiation and target inclinations at shallow angle. However, for a fusion power plant, even higher heat fluxes are to be expected if full detachment is not always achieved. Especially for conventional, actively cooled PFCs, the risk of failure (e.g. loss-of-coolant accidents) dramatically increases with incident heat flux and operation duration. For DEMO this is an even more critical issue. Hence, there is a strong motivation to consider alternative heat exhaust concepts for reactor type devices.

Various alternative target concepts have been proposed. Prominent examples are liquid targets [10], moving belt concepts [11,12] or tungsten dust [13]. A prominent class of concepts relies on utilizing a stream of cascading pebbles [14–17]. Following [17], the key idea of a pebble concept is that pebbles cascade due to gravity through the fusion reactor, thereby providing a primary divertor target surface which intercepts the divertor particle energy, leading to a temperature rise in the pebbles. Once the pebbles are removed from the machine, the heat can be extracted from the pebbles, e.g. by fluidized bed heat exchangers. Then the pebbles can be processed, moved by pneumatic conveyors and

* Corresponding author at: Forschungszentrum Jülich GmbH, Institut für Energie- und Klimaforschung — Werkstoffstruktur und -eigenschaften, 52425 Jülich, Germany.
E-mail address: n.gierse@fz-juelich.de (N. Gierse).

http://dx.doi.org/10.1016/j.nme.2015.01.001

then re-inserted for a next pass through the machine. Pebble concepts have the advantage of separating the heating of the material from the heat removal and allowing additional processing stages, like dust extraction, to be carried out independently from plasma operation. Also pebbles can be replaced during operation, therefore dramatically easing the PFC life time requirements.

However, these features come at the cost of increased complexity and the geometric optimization of shallow angle incidence of $q_{\parallel}$ is lost. The minimum achievable field line inclination angle for conventional PFCs is predicted to be above 2° due to reasons of tile alignment [7]. Assuming an inclination of $\lesssim 3°$ pebble concepts must therefore be able to withstand a heat flux increased by a factor 20, e.g. $q_{\parallel} = 200$ MW/m^2 to compete against an inclined component able to withstand 10 MW/m^2.

With different pebble materials proposed, the use of coatings on pebbles is foreseen to fine-tune the material properties in direct contact with the vessel and plasma and potentially even allow for particle exhaust [18].

In the work presented here, the use of ferromagnetic pebbles for heat exhaust is investigated. In [15], the use of coated ferromagnetic balls of 1 kg weight in a tokamak was investigated for heat removal. It was found that as long as the temperature of the spheres stays below the Curie temperature T_{Curie}, the pebble trajectories can be controlled into orbit-like trajectories by magnetic fields. Also, the idea of magnetic conveyors for the balls is discussed. However, no analysis of the transient heating process of the individual pebble is performed and thus no criterion for optimum pebble size as a function of $q_{\parallel}$ is obtained. Also, the requirement of the pebble temperature to stay below T_{Curie} leads to a high required mass flow of the system and instability of the system. In case of temperature excursion the pebble orbits are uncontrolled if ferromagnetism is lost for temperatures above T_{Curie}, endangering plasma operation in this concept.

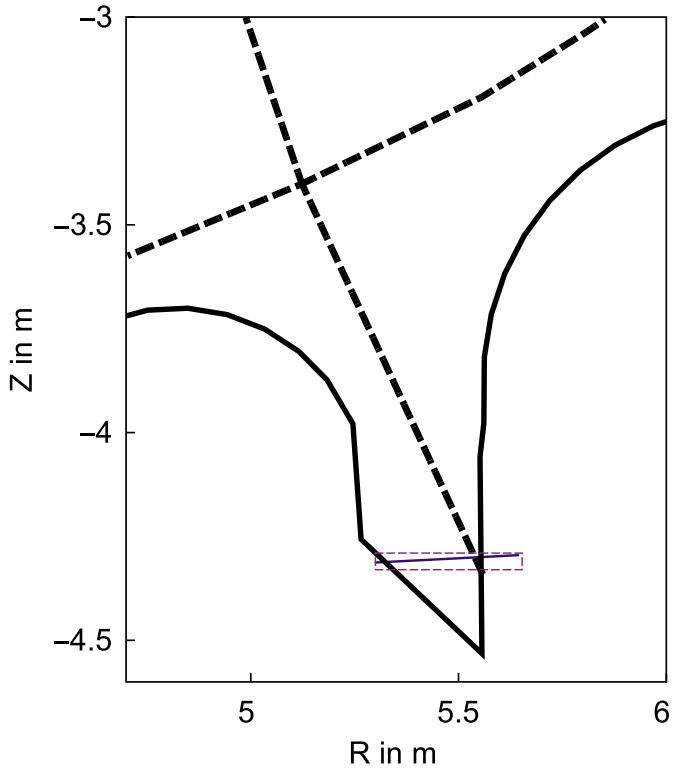

Fig. 1. Schematic setup for ferromagnetic pebbles in an ITER-like machine. The poloidal cross section of the outer lower divertor is shown. Machine wall is shown as solid black line, LCFS as dashed black line and pebble trajectory in blue. Pebbles are released on the outward side and are accelerated inwards by the magnetic gradient force and downwards by gravity. The resulting pebble trajectory of an unheated pebble is indicated in blue. After passing the region of high heat flux the pebbles are collected and recirculated.

A schematic illustrating our proposed approach is shown in Fig. 1. In our concept ferromagnetic pebbles are released in a distance D_{req} from the high heat flux region. The gradients of magnetic confinement setups exhibit an accelerating force on the pebbles. As will be calculated below the magnetic acceleration is ~20 times larger than gravity which is used in non-ferromagnetic pebble concepts, allowing ferromagnetic pebble systems to cope with higher heat fluxes.

After the acceleration phase the pebbles have gained a required velocity v_{req} to cross the high heat flux region. In this region heating of the pebble occurs and ferromagnetism is lost. Then the pebbles are collected and removed from the machine for heat exchange, processing and re-insertion to repeat the cycle.

As is shown by numerical solution of the equations of motion, this setup has the advantage that there is no requirement for the pebble temperature to stay below T_{Curie}. By allowing elevated temperatures the required circulated pebble mass is reduced. Also such a system has a larger margin of error as the pebble trajectories are stable even in case of temperature excursions.

As the general concepts for non-ferromagnetic pebble concepts remain applicable the pebble concept advantages are retained. In addition, ferromagnetic materials dramatically simplify handling of the pebble cycle, as localized magnetic fields opposed to pneumatic conveyors can be used and dust collection and handling of broken pebbles is also dramatically eased.

To investigate our proposed concept we choose the following criteria for the heating process of the pebble:

- CI: No part of the pebble must exceed a material dependent maximum temperature T_{max}. A time t_{max} is defined as the time at which the hottest part of the pebble subject to a heat flux $q_{\parallel}$ reaches T_{max}.
- CII: For an efficient use of the pebble's mass for heat removal the coldest part of the pebble must have been significantly heated before the pebble is extracted. For the following calculations we chose the Curie temperature of the material, T_{Curie} as the desired temperature. The associated time at which the coldest part of the pebble exceeds T_{Curie} is t_{Curie}.
- CIII: The pebble should be exposed to the heat flux for the time t_{Curie} for optimum use of the moved pebble mass for heat exhaust. $t_{\mathrm{rem}} = t_{\mathrm{max}} - t_{\mathrm{Curie}}$ is the safety margin for pebble removal and should be maximized, with $t_{\mathrm{rem}} = 0$ being the limiting case.

The outline of this paper is as follows: The required properties of suited ferromagnetic materials for fusion application are discussed in Section 2. A suitable material concept based on Fe and Cr is chosen as a first candidate material and the compatibility of ferromagnetic pebbles with plasma operation is discussed. In Section 3 the transient heating process by a given heat flux $q_{\parallel}$ is investigated. From the analysis and the criteria set out in the introduction scaling relationships for pebble size, heating and removal time as a function of the incident heat flux $q_{\parallel}$ onto the pebble are found. In Section 4 the removal mechanism due to acceleration in an ITER-like machine is studied. The required "release distance" to the region of impinging heat flux is determined as a function of $q_{\parallel}$ and λ_q. Pebble trajectories for a $q_{\parallel} = 500$ MW/m^2 system are presented and the implications for fusion reactor use of a ferromagnetic pebble system are discussed.

2. Pebble material considerations

For a heat exhaust concept a maximum operation temperature T_{max} as high as possible is desired while the Curie temperature T_{Curie} should be sufficiently low to allow for a large operation window $T_{\mathrm{max}} - T_{\mathrm{Curie}}$. High thermal conductivity is required to prevent large temperature gradients to arise within the pebble.

The use of pure iron is unfavorable due to the bad oxidation resistance and poor mechanical properties. Moreover, the $\alpha-\gamma-$ phase

transition (ferrite to austenite) takes place at 911 °C, which leads to a change in crystallographic structure, namely cubic body centered to cubic face centered. This results in a sudden change of material properties and pebble volume at this temperature, which leads to internal thermal stresses and thermal fatigue. By alloying pure iron with other elements, the $\alpha-\gamma$ – phase transition has definitely to be avoided. At the same time, transmutation of elements and material embrittlement due to neutron damage has to be taken into account by choosing a suited alloying concept. Thus only a few elements can be considered as candidates for alloying iron, like Cr, Ti, Mn, V and C. Taking into account that a feasible material concept for application of ferritic steels in fusion with EUROFER 97 (based on iron, chromium and carbon) already exists [19], a similar material concept is proposed in this paper. Two main changes in comparison to the EUROFER 97 concept are required:

1. The carbon content has to be reduced since it leads to chromium carbide formation and/or austenite formation.
2. The chromium content has to be increased, because the chromium content of EUROFER 97 is not sufficient in order to avoid the $\alpha-\gamma$ – phase transition completely according to the iron – chromium phase diagram [20, Fig. 100].

Thus we propose using an iron–chromium steel with a least 15% chromium, a very low carbon content and no other alloying elements. Such a steel grade standard with exactly this specification does not yet exist. Therefore, for finite element calculations, a similar steel grade with well known temperature dependent thermal material properties up to 1200 °C is used. The steel grade 1.4510 (according to DIN EN 10 088-2) with 16–18% chromium content is commercially available [21] and its alloying concept is close to the above mentioned requirements. The chemical composition in percent by weight according to [21] is reported in Table 1.

Since the pebbles are not used as structural materials, it is considered to be possible to apply this or a similar ferritic steel grade above the usually considered temperature limit of ~700 °C for ferritic steels. Temperature dependent flow stress values of the steel grade 1.4510 up to 1200 °C are available in literature. The flow stress value is approximately 35 MPa at 1200 °C [22]. The Curie temperature is $T_{\mathrm{Curie}} \approx 700$ °C for a binary alloy with this chromium concentration [20].

Moreover, high chromium contents are also favorable in terms of oxidation resistance. Further optimization of the sketched alloying concept is needed. Vanadium, which is considered for fusion reactor use [23] and titanium, avoid the $\alpha-\gamma$ – phase transition at lower concentrations than chromium, leading to an increase in thermal conductivity. Vanadium leads to an increase in Curie temperature, while titanium leads to a decrease.

Additionally, the alloying concept has to be improved with respect to suitable coatings and their application limits. For example, tungsten coatings on the pebble material should be considered to benefit from the low sputtering yields of tungsten.

Furthermore, creep properties and the resulting plastic deformation at high temperatures below yield strength have to be considered and addressed experimentally for the applied external loading conditions in a pebble concept. In case of too large creep deformation there might be a necessity to replace the spheres from time to time during operation. It remains to be investigated to which extend results from ceramic pebble experiments [24,25] and modeling [26] can be applied to steel pebbles. It should be mentioned here that even deformed or destroyed pebbles would still have the benefit of being easily transported by the magnetic force.

Table 1
Chemical composition of steel grade 1.4510 in percent by weight from [21].

	C	Cr	Ti	Mn
Min.	–	16.0	$4 \cdot (C + N) + 0.15$	–
Max.	0.05	18.0	0.80	1.0

Finally, results on the influence of neutron irradiation on ferromagnetic properties for fusion conditions do not yet exist to our knowledge. Experiments in fission reactors on ferrites did not show a significant influence of neutron damage on the Curie temperature [27]. Nevertheless, the influence of neutrons on ferromagnetic properties remains to be investigated for fusion conditions.

For this work steel grade 1.4510 is chosen based on the considerations outlined above. The material properties reported in [22] are used and $T_{max} = 1200$ °C and $T_{\mathrm{Curie}} = 700$ °C are assumed.

2.1. Compatibility of ferromagnetic pebbles with plasma operation

Tokamak discharges can be subject to locked mode instabilities which cause disruptions when the critical relative resonant error field for poloidal mode number, $m \approx 2$ and toroidal mode number $n = 1$, B_{r21}/B_T, exceeds a machine-dependent value, e.g. $\approx 1 \times 10^{-3}$ for COMPASS-C, $\approx 2 \times 10^{-4}$ for DIIID [28] and $\approx 1 \times 10^{-4}$ for JET [29]. Thus the compatibility of ferromagnetic pebbles with plasma operation must be considered. To this goal the magnetic perturbation of the vacuum magnetic field due to a volume filled with ferromagnetic material in the medium-size tokamak TEXTOR [30] has been numerically computed. The finite-element analysis software ANSYS [31] was used for the simulation. TEXTOR was chosen as its $B_{\max} = 3$ T is smaller than the magnetic field strength found in reactor designs, but strong enough to provide magnetic saturation of the inserted material, thereby allowing for an upper estimate of the disturbance. The relative disturbance of the equilibrium field caused by the ferromagnetic insert is given by the field ratio

$$\frac{\delta B}{B}(\mathrm{x}) = \frac{\left|B_{\mathrm{equil}}(\mathrm{x}) - B_{\mathrm{insert}}(\mathrm{x})\right|}{\left|B_{\mathrm{equil}}(\mathrm{x})\right|},$$

with $B_{\mathrm{equil}}(\mathrm{x})$ being the TEXTOR equilibrium magnetic field computed for the flat-top phase of a standard operation scenario without ferromagnetic insert and $B_{\mathrm{insert}}(\mathrm{x})$ the perturbed magnetic field due to the presence of a ferromagnetic insert. A solid cube with an edge length a made from EUROFER 97 is used. $^{\delta B}/_{B}(\mathrm{x})$ is an upper limit for the critical relative error field B_{r21} / B_T. The threshold value of the relative field disturbance is taken as 1×10^{-4}, similar to the threshold used in the description given in [32].

It is found that the length scale of the perturbation is proportional to the insert size a, not to its volume. The strongest influence of the insert is observed in the toroidal direction. For the perturbation to be below the threshold value a required distance to the insert of $<10a$ is found to be required. As will be shown below for a ferromagnetic pebble concept the required vertical distance of the region in which ferromagnetic pebbles are moved will be <10 cm, thus requiring a distance in vertical direction to the last closed flux surface (LCFS) of less than 1 m, which is a feasible dimension for a fusion reactor.

3. Pebble transient heating analysis: optimal diameter and resulting time scales for given $q_{\parallel}$

The transient heating of pebbles must be investigated to determine suited pebble diameters in accordance with criteria CI-CIII for a given heat flux λ_q. If the pebble is too large, strong temperature gradients will arise and the surface temperature will approach $T_{\max}$ before a significant part of the pebble's available heat capacity has been used for heat extraction. In the following the maximum and optimum allowed pebble diameter as a function of $q_{\parallel}$ is determined and the scaling behavior of the relevant timescales is obtained.

The general behavior of the system can be understood from an analytical treatment of transient heating [33]. Assuming a 1d semi-infinite slab geometry with the material extending from the origin to infinity in positive direction, temperature independent material properties

and a uniform material temperature T_0 at the start, an analytical solution for the temperature evolution of the system with a steady state heating power q_{eff} in MW/m^2 is found.

From CI we obtain the maximum allowed exposure time to an effective heat flux density onto the slab surface q_{eff} by demanding that the front of the material may not exceed the maximum allowed temperature T_{max}. A scaling behavior

$$t_{\mathrm{max}}(q_{\mathrm{eff}}) \sim q_{\mathrm{eff}}^{-2} \tag{1}$$

is found with the allowed time a pebble may be exposed to the plasma depending on the inverse square of the plasma heating power.

The scaling of the pebble size is determined by the heat penetration depth at t_{max}. In this simple model 1_{max} describes the depth at which the material temperature exceeds T_{Curie} at t_{max}. For this the scaling relationship

$$l_{\mathrm{max}}(q_{\mathrm{eff}}) \sim q_{\mathrm{eff}}^{-1} \tag{2}$$

is obtained with the length scale proportional to the (linear) inverse of the heat flux q_{eff}.

To investigate the transient pebble heating a numerical simulation of the heating process is carried out. The Transient Thermal package of the finite element software ANSYS 12.0 [31] is used to simulate a spherical pebble made of steel grade 1.4510. The temperature dependent physical properties from [22] are used.

The accurate modeling of the incoming heat flux is a non-obvious question. For dimensions large with respect to the Larmor radius the incident heat flux by charged particles onto a PFC is following the magnetic field line. However, as argued in [16], for millimeter diameter (and smaller) pebbles dissipative processes near the target material become important: finite Larmor radius, neutralization of incident ions and radiation from the plasma lead to dissipative processes resulting in a homogenization of the incoming heat flux. In [17] it is concluded that additionally, the rotation of pebbles leads to a uniform distribution of the heat flux over the full surface area of the sphere. Following the more conservative assumption from [16], we assume a uniform distribution of the heat flux on the plasma-facing hemisphere. As the hemisphere's surface area is twice the sphere's cross section area the pebble surface heat flux density q_{eff} is half of the incident heat flux along the magnetic field line $q_{\parallel}$. The pebble is assumed to be thermally insulated. Most notably thermal radiation off the pebble's surface is neglected as the maximum radiation emitted according to the Stefan–Boltzmann law for a black body at 2000 K is <1 MW/m^2. This is much smaller than the incident heat fluxes considered.

We assume the accuracy of the following analysis to be predominantly limited by the simplifying physical assumptions stated above and not by the numerical errors of the applied methods, which are in excellent agreement with test runs for which analytical solutions are available. Therefore, no uncertainties are reported for the obtained results.

A typical simulation result is shown in Fig. 2. Here $q_{\parallel} = 50$ MW/m^2 and a pebble diameter $d = 0.75$ mm is chosen. For these parameters three times are obtained from the simulation in accordance with CI and CII. t_{max} denotes the time when the hottest part of the sphere exceeds $T_{\mathrm{max}} = 1200$ °C. t_{Curie} marks the time when the coldest part of the pebble exceeds $T_{\mathrm{Curie}} = 700$ °C. This is also the optimum dwell time for a pebble to be exposed to the heat flux, as this indicates that the pebble mass is efficiently used for heat removal. Finally, the safety margin additionally available for removal of the pebble is defined as $t_{\mathrm{rem}} = t_{\mathrm{max}} - t_{\mathrm{Curie}}$. Only pebble diameters which yield $t_{\mathrm{rem}} > 0$ can be used for a given heat flux. Otherwise, the pebble mass could not be fully used for heat removal without melting of the hottest part of the pebble. t_{rem} should be maximized to allow for a safety margin for pebble operation.

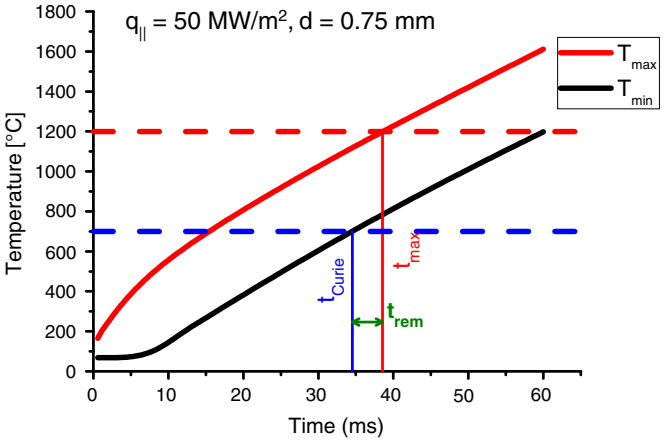

Fig. 2. Numerical simulation results for the hottest part of the pebble $T_{\mathrm{max}}(t)$ and the coldest part of the pebble $T_{\mathrm{min}}(t)$ of a 0.75 mm diameter pebble heated by $q_{\parallel} = 50$ MW/m^2.

To determine which pebble diameter d is suited to remove a given heat flux $q_{\parallel}$ and to determine how the time scales t_{max}, t_{Curie} and thus t_{rem} change as a function of heat flux and pebble diameter, simulation runs with different pebble diameters d are performed for $q_{\parallel} = 10$, 100, 400 and 800 MW/m^2. For each diameter the time scales are determined. An example for $q_{\parallel} = 10$ MW/m^2 is shown in Fig. 3. For each value of the pebble diameter d the time scales t_{max}, t_{Curie} and t_{rem} are obtained. The maximum allowed pebble diameter d_{max} (indicated in magenta) is defined in the limiting case when $t_{\mathrm{max}} = t_{\mathrm{Curie}}$, leading to $t_{\mathrm{rem}} = 0$ s.

As can be seen from the graph, t_{rem} has a weak maximum. Thus there is an optimum diameter $d_{\mathrm{opt}}(q_{\parallel})$ at which t_{rem} has its largest value. d_{opt} is indicated by the dashed blue line. It is at about half the value of d_{max}.

Repeating these simulations for the other values of $q_{\parallel}$ allows us to determine a scaling for the two diameters d_{max} and d_{opt}, as well as the relevant times t_{max}, t_{Curie} and t_{rem}. As discussed for the analytical case the diameter is expected to scale proportional to $q_{\parallel}^{-1}$ and the time scales are expected to scale with $q_{\parallel}^{-2}$. In Fig. 4 the fit results for the diameters are shown. The results are

$$d_{\mathrm{max}}[\mathrm{mm}] = 42.59\, q_{\parallel}^{-1} \tag{3}$$

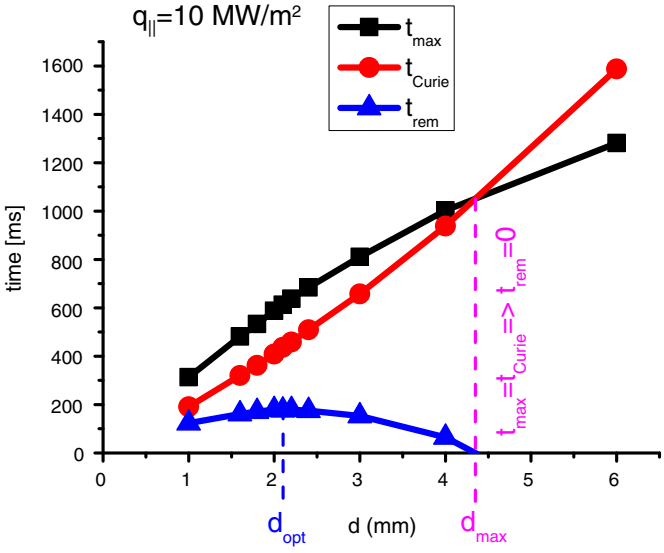

Fig. 3. Time scales t_{max}, t_{Curie} and t_{rem} obtained for different pebble diameters for $q_{\parallel} = 10$ MW/m^2.

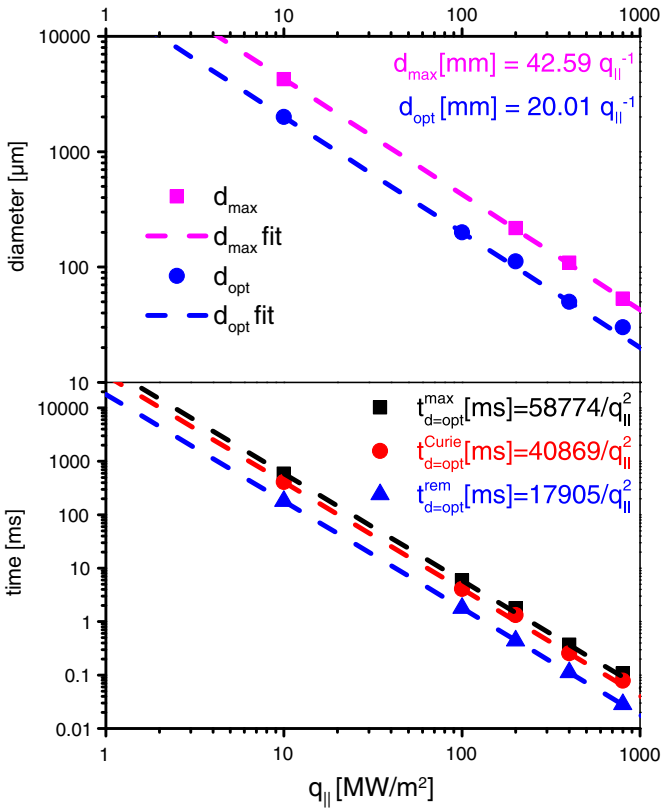

Fig. 4. Pebble transient heating result as a function of $q_{\parallel}$. Top: d_{opt} and d_{max} as a function of $q_{\parallel}$. Bottom: t_{max}, t_{Curie} and t_{rem} as a function of $q_{\parallel}$.

and

$$d_{opt}[\mathrm{mm}] = 20.01\, q_{\parallel}^{-1}. \tag{4}$$

Likewise, the scaling for t_{max}, t_{Curie} and t_{rem} is determined to be (with $q_{\parallel}$ in MW/m^2)

$$t_{max}^{d_{opt}}[\mathrm{ms}] = 58774\, q_{\parallel}^{-2} \tag{5}$$

$$t_{Curie}^{d_{opt}}[\mathrm{ms}] = 40869\, q_{\parallel}^{-2} \tag{6}$$

$$t_{rem}^{d_{opt}}[\mathrm{ms}] = 17905\, q_{\parallel}^{-2}. \tag{7}$$

The computed data is shown together with the obtained fitting results in Fig. 4.

4. Ferromagnetic pebbles in an tokamak fusion reactor

4.1. Steady state heat flux removal capabilities

In a tokamak machine the heat flux $q_{\parallel}$ impinges onto the PFCs intersecting the field lines within the power decay length λ_q. From the scaling relationships obtained in Section 3 the pebble parameters can be determined for a given heat flux $q_{\parallel}$. The pebbles should be exposed to the region in which the heat flux is present until the coldest part of the pebble reaches the Curie temperature. The ideal duration for exposure is known by $t_{Curie}^{d_{opt}}(q_{\parallel})$ from the above scaling. We can now compute a required pebble velocity $v_{req}(q_{\parallel}, \lambda_q)$ for the pebbles to cross the region of the power decay length. For simplicity, we assume that the heat flux $q_{\parallel}$ impinges uniformly over the whole distance λ_q in the poloidal plane in the divertor region and we limit our analysis to the outer divertor leg, as the highest heat fluxes are observed here. The required velocity of the pebble to cross the distance in which the heat flux is present within $t_{Curie}^{d_{opt}}$ is given by

$$v_{req} = \frac{\lambda_q}{t_{Curie}^{d_{opt}}(q_{\parallel})}. \tag{8}$$

As the pebbles are ferromagnetic, v_{req} can be obtained from releasing the pebbles at a release distance D_{req} away from the heat flux region. To determine D_{req} we must compute the pebble acceleration due to the magnetic gradients inside a tokamak.

Acceleration of the pebbles can be provided by the magnetic gradient force onto the ferromagnetic pebble. The acceleration due to a magnetic gradient in a toroidally symmetrically setup is given by

$$\mathbf{a}_{mag} = \frac{1}{m_{pebble}} \nabla(\mathbf{m}\cdot\mathbf{B}) = M_S[(\nabla_r B_r)\hat{\mathbf{e}}_{\mathbf{r}} + (\nabla_z B_z)\hat{\mathbf{e}}_{\mathbf{z}}]. \tag{9}$$

Here m_{pebble} denotes the pebble mass and M_S the saturation magnetization per mass of the pebble material. For numerical values the properties reported for EUROFER 97 [19], $M_S = 180$ A m^2/kg, is used. As in the case of acceleration by gravity ($g = 9.81$ m/s^2) the magnetic acceleration is independent of pebble mass and only depends on the saturation magnetization per mass of pebble material M_S.

For a tokamak configuration the gradients in the z-direction are negligible compared to the radial direction. Thus the magnetic acceleration of a pebble in radial direction is approximated by

$$a_{mag} = M_s \nabla_r B_r. \tag{10}$$

In a tokamak the strength of the magnetic field as a function of major radius can be described by $B_r(R) = B_0 R_0/R$ and thus the magnetic gradient is given by $\nabla_r B_r = -B_0 R_0/R^2$, with the on-axis values $R_0 = 6.21$ m and $B_0 = 5.3$ T for an ITER-like machine. From Eq. (10) the acceleration of a pebble is calculated. The acceleration will be inward and is much stronger than the acceleration due to gravity and increasing towards the center. The range for ITER is $a_{mag}(R = 7\ \mathrm{m}) = 12.3$ g far outside and increasing up to $a_{mag}(R = 3.0\ \mathrm{m}) = 67$ g further inwards. For the following calculations we use the acceleration $a_{mag} \approx 18.6$ g at the location outside of the outer divertor, $R = 5.7$ m.

With the known acceleration the required release distance along the major radius is given by

$$D_{req}\left(q_{\parallel}, \lambda_q\right) = \frac{v_{req}^2}{2\, a_{mag}}.$$

The solutions for D_{req} in cm are presented as a function λ_q for different values of $q_{\parallel}$ in Fig. 5. Counter-intuitively, this result shows that the ferromagnetic pebble heat removal capability increases for a given release distance as λ_q decreases.

To replace a static PFC which can withstand a surface heat flux of 10 MW/m^2, $q_{\parallel} = 200$ MW/m^2 is required for our pebble system. The pebble parameters $d_{opt} = 100$ µm, $t_{max}^{d_{opt}} = 1.46$ ms, $t_{Curie}^{d_{opt}} = 1.02$ ms and thus $t_{rem}^{d_{opt}} = 0.44$ ms follow from above scaling relationships. For $\lambda_q = 3$ mm a required release distance of 2.36 cm is found. If a shorter decay length $\lambda_q = 1$ mm is assumed a release distance of only 0.26 cm is required.

We want to point out that this is fundamentally different from the behavior of static PFCs which are cooled by thermal diffusion and therefore have an absolute limitation in allowable heat flux, independent of λ_q. This result shows that our concept performs better in case of short power decay lengths and in particular very high values of $q_{\parallel}$ are accessible for systems with λ_q approaching 1 mm.[1]

[1] Note, however, that in the overall power balance there is a relationship between the parallel heat flux across the separatrix $q_{\parallel sep}$ and λ_q, namely $q_{\parallel sep} \sim p_{sep} / (R\ \lambda_q\ B_p / B_t)$ [7] so that the reduction of λ_q imposes a higher value of $q_{\parallel,sep}$. However, as also discussed in [7] extrapolation from $q_{\parallel,sep}$ to the resulting heat flux on the PFCs is not possible at present.

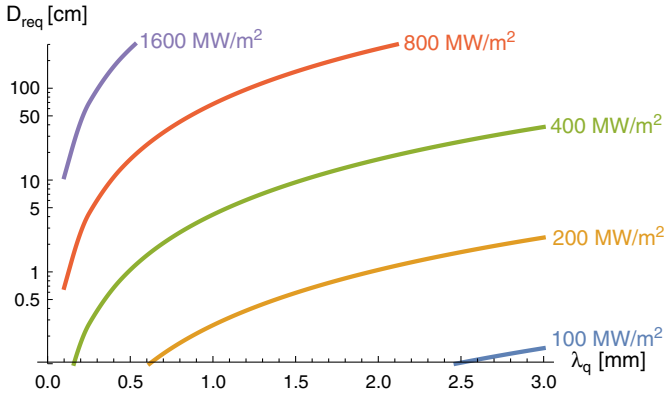

Fig. 5. Required pebble release distance D_{req} as a function of power decay length λ_q at pebble location for different $q_{\parallel}$ values. If the pebbles are released at least D_{req} from the heat flux region, removal within $t_{Curie}^{d_{opt}}(q_{\parallel})$ is achieved. Note that the ferromagnetic pebble concept performs best for short values of λ_q.

For $q_{\parallel} = 500$ MW/m^2 (corresponding to a hypothetical static PFC able to withstand a heat flux of 25 MW/m^2) the system parameters $d_{opt} = 40$ μm, $t_{max}^{d_{opt}} = 235$ μs, $t_{Curie}^{d_{opt}} = 163$ μs, $t_{rem}^{d_{opt}} = 72$ μs and $D_{req}(\lambda_q = 1\ \text{mm}) = 10.3$ cm are found.

4.2. Pebble trajectories

To study the behavior of such a system and especially the effect of loss of ferromagnetism when heated the pebble trajectories must be computed. A simulation of the pebble trajectory for the aforementioned $q_{\parallel} = 500$ MW/m^2 case is shown in Fig. 6. The pebble is injected at rest at t_0 at $R_{start} = 5.643$ m, $Z_{start} = -4.295$ m. The pebble trajectory due to gravity and the magnetic acceleration $a_{mag}(R)$ described above is then numerically computed using the Mathematica software [34]. Graph a) shows a magnification of the area indicated by the magenta frame in Fig. 1. The pebble position of the cold pebble at t_0 is indicated by a blue circle. The resulting trajectory for the cold pebble is shown in gray. Additionally, every $\Delta t = 3$ ms the pebble location is indicated by a blue circle. The acceleration inwards due to the magnetic force and downwards due to gravity can be seen.

We assume the heat flux onto the pebble to be negligible ($\ll 500$ MW/m^2) outside the λ_q-region. As the pebble approaches the high heat flux region (indicated by the dashed black line) it is heated as discussed in Section 3. The details of the heating process inside the λ_q-region are involved and require e.g. a detailed knowledge of the actual λ_q profile. Therefore, two limiting cases are investigated: the trajectory of an unheated pebble is shown in gray. The red circles show the trajectory of a pebble which is instantaneously heated above T_{Curie} on entering the λ_q-region. The actual pebble trajectories will be between these two cases.

As to be expected it can be seen from the spacing between the respective circles in the graph that the absence of further magnetic acceleration leads to a stronger downward-bend of the hot pebble trajectory and a slower final velocity.

In part b) a magnification of the λ_q-region (shown as a light red area) is shown. $\lambda_q = 1$ mm is assumed. Notice the small aspect ratio of the graph. The same color code and method as in a) was used. However, now the pebble location is shown for the 300 times shorter time step $\Delta t = 10$ μs. In accordance with the computations of the previous section the hot pebble crosses the λ_q region in 163 μs, corresponding to 16 circles in the graph. On the length scale of 1 mm almost no difference between the heated and the cold sphere can be observed on the relevant short distance. This illustrates that the inertia acquired by releasing the pebble at D_{req} is sufficient to guide the pebble on the course with marginal scattering of the pebble arrival point at the collection system.

To investigate the system's stability against material deterioration or statistical distribution of pebble magnetic properties, the case of a pebble with decreased magnetic properties (assumption $M_{S,damaged} = 0.99\ M_S$, pebble mass unchanged) is shown. The difference in trajectory to the original pebble is not visible on the large scale of graph a). On the scale of λ_q, shown in b), an advantage of the concept can be seen. Even the slight deterioration of the magnetic property leads to the pebble trajectory being recessed more than one pebble diameter from the impinging heat flux. This is an additional safety mechanism: if a distribution of pebbles with different magnetic properties is injected the ones with the largest magnetic moment density to mass density ratio will obtain the highest velocity in radial direction and face the harshest conditions, while pebbles with deteriorated magnetic properties will be shielded by pebbles with better magnetic moment/mass density ratio. This stable behavior provides a passive safety mechanism and is an advantage compared to the vicious circle in tile alignment procedures where damage of

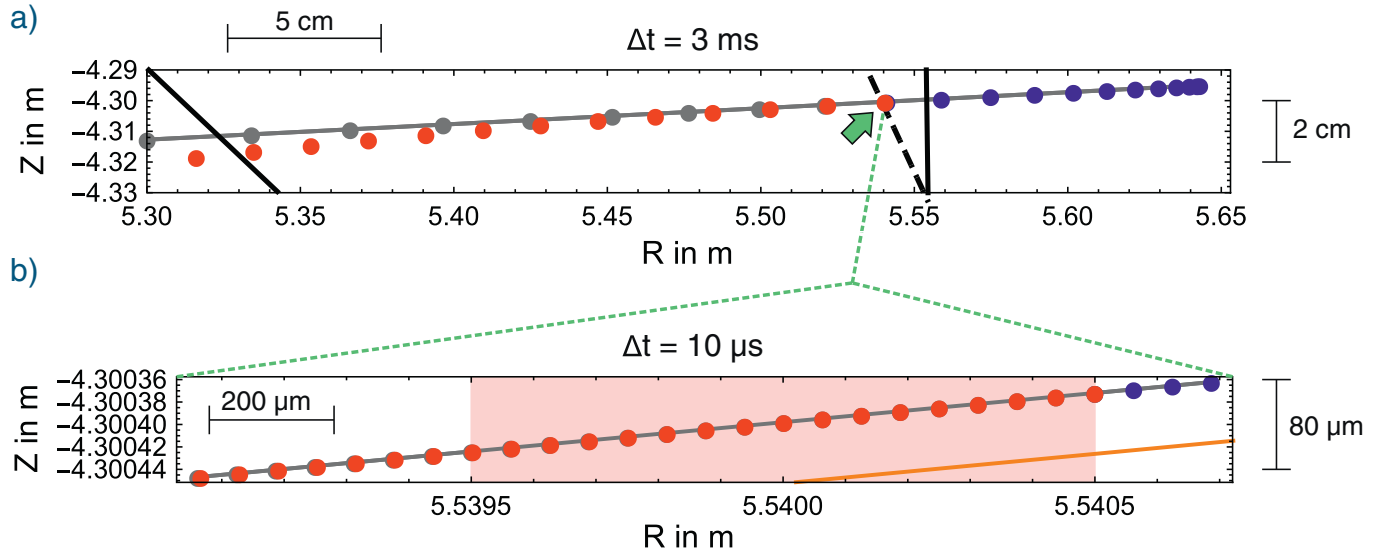

Fig. 6. Numerical simulation of the pebble trajectories. Pebble position for each time step Δt is shown. a) Injection of cold pebbles (blue), acceleration remotely from the plasma, heating in the high heat flux area (black dashed line). Hot pebble trajectory indicated by red circles, cold pebble trajectory by solid gray line and blue and gray circles. b) Magnification of the high heat flux region (light red area), $\lambda_q = 1$ mm. Instantaneous heating is assumed. Additionally, the trajectory of a slightly damaged cold pebble ($M_{S,damaged} = 0.99 \cdot M_S$) is shown in orange.

the tile surface can lead in turn to a steeper angle of incidence at the damaged surface.

4.3. Required pebble mass circulation

In the following the required amount of pebble material is estimated. When assuming D-T fuel, 1/5 of the thermal heat output P_{th} is released as $\alpha-$particles which lead to the heat load on the PFCs along the magnetic field lines: $P_{wall} = 0.2P_{th}$. Assuming that the pebble temperature at the time of removal exceeds the Curie temperature $T_{Curie} \approx 700$ °C of our candidate material the pebble mass flow can be estimated conservatively by assuming that the pebble is heated from a starting temperature T_0 to T_{Curie} uniformly. We arbitrarily assume $T_0 = 68$ °C for the calculation, leading to a temperature increase $\Delta T = 632$ K. With a volumetric heat capacity for 700 °C [22] the required mass flow is then given by

$$\dot{\rho} = 517\, P_{th}^{GW} \ \text{kg/s}. \tag{11}$$

Here P_{th}^{GW} is the total thermal fusion power in GW. For a $P_{th}^{GW} = 3$ reactor this leads to a required mass flow rate of 1551 kg/s. This is in the same range as found in cascading (non-ferromagnetic) pebble concepts proposed earlier, e.g. 900 kg/s proposed in [17]. A detailed investigation of the electrical power required to maintain the required mass flow rate needs to be performed in future work. However, a crude scaling can be made based on existing technology, e.g. in mining industry, where much larger steady state mass flows are routinely established, resulting for a $P_{th} = 3$ GW reactor in a required electrical power of 9.2 MW.

Assuming a thermal conversion efficiency of 1/3 this is less than 1% of the electrical power output of such a fusion reactor. We therefore conclude that the mass circulation required for our concept does not endanger the fusion reactor power balance.

4.4. Pebble inventory considerations

Assuming that the pebbles remain inside the machine for $\lesssim 250$ ms (a very conservative assumption as this is twice t_{max} for $q_{\parallel} = 20$ MW/m^2 and found to be much shorter for relevant values of $q_{\parallel}$) this would lead to a steady-state inventory of $\lesssim 400$ kg ferromagnetic material inside the vacuum vessel.

The required steady state inventory amounts to less than one quarter of the typical structural steel mass proposed for different ITER test breeding module (TBM) designs [35, see Table 1 for an overview of proposed structural steel requirements] and could be distributed quasi-symmetrically along the torus to minimize the effect on plasma operation.

5. Summary

In this work ferromagnetic pebbles for heat exhaust in fusion reactors with short power decay length are considered on a conceptual level. The reasons to choose steel grade 1.4510 as a candidate material are the Fe–Cr composition and the availability of material data.

For this candidate material a numerical transient thermal analysis of pebble heating by a parallel heat flux $q_{\parallel}$ is performed. General scaling relationships for the maximum allowed pebble diameter $d_{max}(q_{\parallel})$ and the optimum pebble diameter $d_{opt}(q_{\parallel})$ are obtained. For $d_{opt}(q_{\parallel})$ the maximum allowed exposure time $t_{max}(q_{\parallel})$ and optimum exposure time $t_{Curie}(q_{\parallel})$ are obtained. For $q_{\parallel} = 200$ MW/m^2, corresponding to a static target with 3° inclination to the field lines with a heat flux of 10 MW/m^2, the values $d_{opt} = 100\ \mu$m, $t_{max}^{d_{opt}} = 1.46$ ms, $t_{Curie}^{d_{opt}} = 1.02$ ms are found.

A possible implementation concept for heat removal for an ITER-like machine is outlined in which the inward acceleration of the ferromagnetic pebbles due to the gradient of the magnetic field strength is used to exchange the pebbles. The required release distance D_{req} of the pebble to the open field lines is determined as a function of $q_{\parallel}$ and λ_q. Counter-intuitively we find that the pebble system's heat removal capability increases as λ_q decreases.

For $\lambda_q = 3$ mm a value of $D_{req} = 2.36$ cm is found, while for $\lambda_q = 1$ mm only $D_{req} = 0.26$ cm is needed.

For narrow λ_q profiles the proposed system is able to cope with heat fluxes exceeding the parameter space accessible by static PFCs, e.g. for $q_{\parallel} = 500$ MW/m^2 (corresponding to 25 MW/m^2 heat flux on a static target) $d_{opt} = 40\ \mu$m diameter and $D_{req} = 10$ cm are found. This suggests that ferromagnetic pebble concepts are particularly well suited in case of narrow heat flux profiles and strong magnetic gradients, found in low aspect ratio tokamaks. Numerical simulations of pebble trajectories are performed. It is shown that operation above T_{Curie} does not affect the pebble trajectory in the λ_q region significantly and only leads to a pebble deflection <10 cm in vertical direction far away from the high heat flux region.

Additionally, a passive safety property of the concept which leads to sorting of pebbles according to their magnetic properties is described.

The required pebble mass flow for a $P_{th} = 3$ GW fusion reactor is found to be ~1600 kg/s. It is estimated that less than 1% of the electrical power output of such a fusion reactor is required to maintain the pebble mass flow which is seen as uncritical to the overall power balance of the fusion reactor. The steady state inventory of ferromagnetic material is $\lesssim 400$ kg, less than one quarter of the typical structural steel mass proposed for different ITER test blanket module designs. By finite element analysis it is shown that ferromagnetic pebbles are compatible with plasma operation. Here more detailed analyses of the effects of moving pebbles as well as on collective effects of ferromagnetic pebbles in magnetic fields are required.

The detailed dynamics of the pebbles, the effect of pebble motion on magnetic perturbations and pebble interaction effects, as well as additional forces on small diameter pebbles remain to be investigated.

This analysis shows that ferromagnetic pebbles are suitable for high heat flux scenarios with narrow λ_q profiles which are not accessible to the operational range of conventional PFCs. We conclude that ferromagnetic pebbles are an interesting heat exhaust concept to be investigated as an option for heat exhaust in view of DEMO.

Acknowledgments

This project has received funding from the European Union' s Horizon 2020 research and innovation programme under grant agreement number 633053. The views and opinions expressed herein do not necessarily reflect those of the European Commission. We wish to acknowledge helpful discussions with Anton Möslang (KIT) regarding the considerations behind choice and operation limits of ferromagnetic materials in fusion environments. Helpful discussions with Max Baum, Heinke Frerichs, Felix Hasenbeck and Michael Rack are gratefully acknowledged. Finally, we want to thank the two reviewers for their insightful questions, comments and suggestions which significantly added to the quality of this article.

References

[1] J.P. Freidberg, Plasma Physics and Fusion Energy, 1st edition Cambridge University Press, 2008.
[2] G. Federici, P. Andrew, P. Barabaschi, et al., J. Nucl. Mater. 313–316 (2003) 11.
[3] J. Linke, T. Loewenhoff, V. Massaut, et al., Nucl. Fusion 51 (2011) 073017.
[4] J. Roth, E. Tsitrone, A. Loarte, et al., J. Nucl. Mater. 390–391 (2009) 1.
[5] A. Kirschner, A. Kreter, P. Wienhold, et al., J. Nucl. Mater. 415 (2011) S239.
[6] D. Stork, P. Agostini, J. Boutard, et al., J. Nucl. Mater. 455 (2014) 277.
[7] H. Zohm, C. Angioni, E. Fable, et al., Nucl. Fusion 53 (2013) 073019.
[8] A. Loarte, in: R.E. Clark, D.H. Reiter, F. Schäfer, J. Toennies, W. Zinth (Eds.), Nuclear Fusion Research, Springer Series in Chemical Physics, vol. 78, Springer, Berlin Heidelberg 2005, pp. 61–95.
[9] T. Eich, B. Sieglin, A. Scarabosio, et al., Phys. Rev. Lett. 107 (2011) 215001.
[10] M. Ono, M. Bell, R. Bell, et al., Fusion Eng. Des. 85 (2010) 882.

[11] Y. Hirooka, M. Tillack, A. Grossman, Fusion Engineering, 1997, 17th IEEE/NPSS Symposium, vol. 2 1997, pp. 906–909.
[12] Y. Hirooka, H. Fukushima, N. Ohno, S. Takamura, Fusion Eng. Des. 65 (2003) 413.
[13] X. Tang, G. Delzanno, J. Fusion Energy 29 (2010) 407.
[14] S. Mirnov, Sov. J. Plasma Phys. (Engl. Transl.) 6 (1980) 127.
[15] K. Ikuta, A. Miyahara, J. Nucl. Mater. 121 (1984) 374.
[16] M. Isobe, K. Matsuhiro, Y. Ohtsuka, Y. Ueda, M. Nishikawa, Nucl. Fusion 40 (2000) 647.
[17] G. Voss, A. Bond, S. Davis, M. Harte, R. Watson, Fusion Eng. Des. 81 A (2006) 327.
[18] K. Matsuhiro, M. Isobe, Y. Ueda, M. Nishikawa, Fusion Eng. Des. 49–50 (2000) 283.
[19] K. Mergia, N. Boukos, J. Nucl. Mater. 373 (2008) 1.
[20] K. Adachi, Figs. 100 - 126, tables 30 - 34, Landolt-Börnstein - Group III Condensed Matter, volume 19a, 1986 pp. –.
[21] http://www.thyssenkrupp-nirosta.de/fileadmin/scripts/wbbreitband/en/blaetter/4510.pdf (retrieved 2012-02-19).
[22] M. Spittel, T. Spittel, Landolt–Börnstein — Group VIII Advanced Materials and Technologies, vol. 2C1, Springer-Verlag, Berlin Heidelberg, 2009 (pp. –).
[23] J. Smith, W. Johnson, R. Stambaugh, et al., Fusion Engineering, 1995, SOFE '95. 'Seeking a New Energy Era'., 16th IEEE/NPSS Symposium, vol. 2 1995, pp. 858–861.
[24] G. Piazza, J. Reimann, E. Günther, et al., J. Nucl. Mater. 307–311 (Part 1) (2002) 811.
[25] J. Reimann, E. Arbogast, M. Behnke, S. Müller, K. Thomauske, Fusion Eng. Des. 49–50 (2000) 643.
[26] D. Aquaro, N. Zaccari, Fusion Eng. Des. 75–79 (2005) 903.
[27] E.I. Salkovitz, G.C. Bailey, A.I. Schindler, J. Appl. Phys. 29 (1958) 1747.
[28] R.J.L. Haye, R. Fitzpatrick, T.C. Hender, et al., Phys. Fluids B 4 (1992) 2098.
[29] G. Fishpool, P. Haynes, Nucl. Fusion 34 (1994) 109.
[30] O. Neubauer, G. Czymek, B. Giesen, et al., Fusion Sci. Technol. 47 (2005) 76.
[31] ANSYS Academic Research, ANSYS Release 12, ANSYS, Inc., 2009
[32] J. Coenen, O. Schmitz, B. Unterberg, et al., Nucl. Fusion 51 (2011) 063030.
[33] H.S. Carslaw, J.C. Jaeger, Conduction of Heat in Solids, 2 edition Oxford University Press, USA, 1986.
[34] Wolfram Research Inc., Mathematica, Version 10.0.1.0, Wolfram Research, Inc., Champaign, Illinois, 2014. (Place of publication).
[35] L. Giancarli, V. Chuyanov, M. Abdou, et al., J. Nucl. Mater. 367–370 (Part B) (2007) 1271.